Penerbit Akademia Baru

Journal of Advanced Research in Fluid Mechanics and Thermal Sciences

Journal homepage: www.akademiabaru.com/arfmts.html
ISSN: 2289-7879

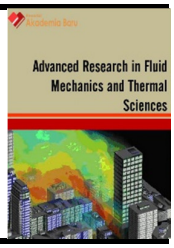

Experimental and Numerical Investigation of Thermosyphon Heat Pipe Performance at Various Inclination Angles

Open Access

Bala Abdullahi[1,2,*], Ahmed El-Sayed[1], Raya Khalid Al-Dadah[1], Sa'ad Mahmoud[1], Abdel Fateh Mahrous[3], Nura Mu'az Muhammad[2], Sa'idu Bello Abbakar[2]

[1] School of Mechanical Engineering, University of Birmingham, Birmingham, B15-2TT, United Kingdom
[2] Mechanical Engineering Department, Kano University of Science & Technology, Wudil, Kano, Nigeria
[3] Mechanical Power Engineering Department, Menoufiya University, 32511, Shebin El-Kom, Egypt

ARTICLE INFO

Article history:
Received 9 March 2018
Received in revised form 6 April 2018
Accepted 25 April 2018
Available online 27 April 2018

ABSTRACT

Interest in the use of heat pipes in solar applications is increasing due to their role in improving the heat transfer performance of solar collectors. In order to effectively utilise heat pipes, their performance under various operating conditions and inclination angles need to be investigated. In this work, numerical and experimental studies were carried out to investigate the effects of heat input and inclination angle on the wall temperature distributions and thermal resistance of thermosyphon heat pipe. A Computational Fluid Dynamics (CFD) model was developed using ANSYS Fluent to simulate the flow and mass transfer using volume of fluid (VOF) approach together with user - defined function (UDF) to simulate the phase change processes at various inclination angles. Experiments were carried out to validate the CFD model at heat inputs of 81.69W and 101.55W with temperature distribution results showing good agreement of ±4.2% average deviation. Also the predicted thermal resistance at different inclination angles showed good agreement with the experimental ones with maximum deviation of ±5.7%. Results showed that as the heat input increases, the heat pipe wall temperature increases and the thermal resistance decreases. Experimental and numerical results showed that increasing the inclination angle will improve the thermosyphon heat pipe performance to reach its maximum value at 90o, but this effect decreases as the heat input increases.

Keywords:
Thermosyphon, Computational Fluid Dynamics, Inclination angle

1. Introduction

Heat pipe is an effective heat transfer device involving simultaneous evaporation and condensation processes. It consists of evaporator and condenser sections with or without adiabatic section in between them. Heat is supplied to the evaporator section where the working fluid evaporates and flows to the condenser section where it condenses to liquid using cooling medium. The condensate returns to the evaporator by capillary effects in case of wicked heat pipe and by gravity in case of wickless heat pipe (thermosyphon).

* *Corresponding author.*
E-mail address: balabdullahi@yahoo.com (Bala Abdullahi)

Heat pipes have many advantages including high heat conduction, light weight, efficient heat transfer and design flexibility. Due to these advantages, the technology has undergone rapid development in the past decades [1] leading to their applications in spacecraft thermal control [2], heat exchangers [3] and solar energy systems [4, 5].

Thermosyphon heat pipes are highly durable and cost effective which make them suitable for various applications such as solar heating of buildings [6] and cooling of turbine blades, transformers, electronics, internal combustion engines and nuclear reactors [7, 8]. This is due to their ability to dissipate and transfer large amount of energy from small area without any significant loss. Some applications of thermosyphon require that the pipe be inclined to an angle from the horizontal [4, 6, 9, 10].

There are many numerical models developed to simulate the performance of thermosyphon under various operating conditions, Experimental and CFD modelling of flow and heat transfer in thermosyphon using volume of fluid (VOF) approach was presented by Asghar *et al*., [11]. The effects of heat inputs and fill ratio on the performance of the heat pipe were investigated using 1000mm long pipe. Results showed that the performance of the thermosyphon increases with the increase in heat input between 350W and 500W, but it decreases when the heat input is above 500W. Also for the fill ratios tested; 0.3, 0.5 and 0.8, the best performance was found at the fill ratio of 0.5. A two- phase model for the flow and heat transfer in a thermosyphon was developed by Asmaie *et al*., [12] by using de – ionized water and mixture of copper(II)oxide with water as working fluid. Temperature distributions on the wall and the heat transfer coefficients of both the evaporator and condenser were predicted. The CFD results were validated with the experimental results reported by Liu *et al*., [13] and were in good agreement especially at the adiabatic and condenser sections. The effects of working fluid type, concentration of nanofluid and inlet heat flux were investigated and results reported showed that the wall temperature of the pipe decreases with increase of the concentration of nanofluid. Also the maximum heat flux of the nanofluid was found to be 46% higher than that of the water.

A three – dimensional CFD model to simulate the flow boiling process of hydrocarbon feedstock heat exchanger of a steam cracker was developed by De Schepper *et al*., [14]. VOF together with user defined function (UDF) were used in modelling the convection section of the cracker. Also the authors proposed correlations for the interphase mass source term used in the governing equations for simulating the evaporation and boiling phenomena in the cracking furnace. CFD model using VOF together with UDF was built to simulate the flow and heat transfer in a two – phase closed thermosyphon by Fadhl *et al.*, [15]. The temperature profiles obtained from the simulation was in agreement with the experiment at high heat input ranging from 275.6 to 376.14W. But there is large deviation between the experimental thermal resistances and the simulation especially at the low heat inputs around 60% at 100.41W. It can be seen that all the reported CFD simulation of thermosyphon heat pipes were carried out with the pipe in vertical orientation, hence none of them consider the situation when it is inclined.

Also ANSYS software has largely been used in simulating heat transfer processes in different channels such as in turbulent circular pipe [16], circular channel with constant heat flux [17] and in rectangular microchannel heat sink [18].

However, considerable experimental research works were published on the investigation of the effects of parameters like the geometry, working fluid, fill factor and inclination on the thermosyphon heat pipe performance [19-23]. Regarding the effect of inclination angle on heat pipe performance, conflicting results were reported like angles between 15^{o} and 60^{o} [22], between 40^{o} and 45^{o} [23] and 60^{o} [24] gave the best performance. Others reported higher angles like 90^{o} [25] and 83^{o} [26] as the best performing angles while some reported that inclination angle has no

effect [27]. Various applications like solar systems require the use of heat pipes in inclined positions from the horizontal which makes the investigation of the inclination angle on heat pipe performance of paramount importance. With the contradictory experimental results in the literature and the lack of any numerical studies on the effect of inclination, this work aims to address these issues by developing a CFD model that takes into account the effect of inclination angles (10^o to 90^o) and experimentally validated the modelling. Hence, this research closes the gap of the effects of the inclination angle of a thermosyphon on its performance and the thermal resistance. This will leads to the selection of best inclination angle for an improved performance of the system.

2. Methodology

Figure 1 shows the experimental test facility consisting of a two – phase closed thermosyphon heat pipe heated electrically at the evaporator section and water cooled at the condenser section. The thermosyphon used is a 400mm long, 22mm outer diameter, 0.9mm thick closed copper tube with water as the working fluid (0.65 fill ratio). It has 200mm long evaporator, 200mm long condenser and no adiabatic section. Uniformly wrapped electrical wire was used to heat the evaporator section using TSx1820P Programmable DC PSU 18V/20A power regulator with accuracy of ± (0.5% + 1 digit) for the current. The voltage was measured using a digital multimeter from Mastech (MAS 343) of 3 3/4 digital display and maximum accounts of 3999 (AC voltage 400V ± 0.5%) which was connected close to the pipe to account for voltage drop. The evaporator section is insulated with 25mm thick pipe insulator to reduce the heat losses to the ambient. The condenser section was cooled using water jacket. The cooling water flow rate was controlled by a valve and measured using an Omega FLR1009ST-I flow meter (50 – 500 mL/min) with measurement uncertainty of ±2.09% of full scale.

Six thermocouples were placed at different locations on the pipe; four and two on the evaporator and condenser sections respectively to measure the wall temperatures. Three thermocouples were used on the water jacket and one on the insulation surface to measure the effectiveness of the insulation. Two probe thermocouples were used to measure inlet and outlet temperatures of the cooling water in the condenser section. The readings were logged using Pico TC - 08 data loggers connected to a PC.

Seven different heat inputs ranging from 20W to 110W were used with an average flow rate of 0.00224 kg/s for the thermosyphon at the vertical position. The values of the heat inputs were obtained from optical simulations on different geometries of compound parabolic concentrators [28, 29].

The power input to the evaporator is calculated from the product of the current, *I* and voltage, *V* supplied thus

$$Q_{in} = VI \tag{1}$$

The effectiveness of the performance of thermosyphon is determined by its overall thermal resistance, R_{th} given by

$$R_{th} = \frac{T_{ae} - T_{ac}}{Q_{in}} \tag{2}$$

where T_{ae} and T_{ac} are the average temperatures on the evaporator and the condenser respectively and Q_{in} is the heat supplied.

The performance of the thermosyphon can also be evaluated in terms of the rate of heat transfer to the cooling water as [11]

$$\eta = Q_{out} / Q_{in} \tag{3}$$

The rate of heat transfer to the cooling water can be determined by

$$Q_{out} = \dot{m} C_p (T_{out} - T_{in}) \tag{4}$$

where $\dot{m}$ is the mass flow rate, kg/s and C_p is the specific heat capacity of water, kJ/kg-K. While T_{in} and T_{out} are the average inlet and outlet cooling water temperatures respectively.

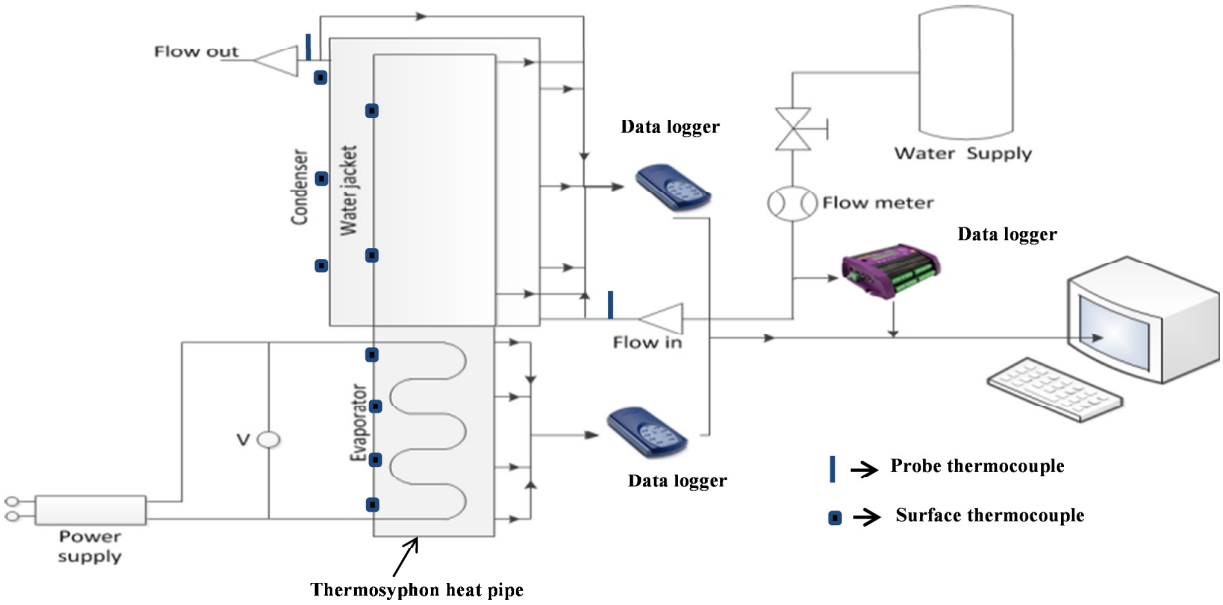

Fig. 1. Schematic diagram of the experimental test rig for thermosyphon characterization

Figure 2 shows the performance of the thermosyphon aligned vertically at different heat inputs. It can be seen from such figure that the performance of the pipe increases as the heat inputs increases from 20 to 81.69W, but it tends to decrease as more heat is supplied showing the limit of this pipe has been reached under these operating conditions. At low heat input, the vapour generated from the evaporator section is small, so there will be significant dry areas in the condenser section; hence heat transfer is largely by free convection. As the heat is gradually increased, more vapours will rise to the condenser section, there will be high condensation rate on the condenser wall and the dominant heat transfer mechanism will be condensation. But at certain high heat input, thick layer of liquid can be formed on the wall of the pipe causing high thermal resistance and hence lower the heat transfer to the cooling water, hence reduction of performance.

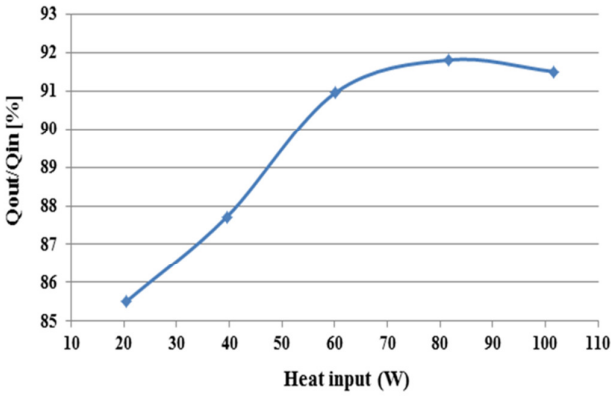

Fig. 2. Performance of thermosyphon aligned vertically at different heat inputs

Figure 3 shows the evaporator and condenser wall temperatures respectively. It can be seen that the temperature distribution is almost uniform for each heat input and this is due to the constant temperature phase change process taking place in the evaporator section (Figure 3 (left)). But on the condenser section, there is rise in the temperature at the top of the condenser which is due to the rise of the saturated steam to the top of the tube and the formation of liquid film layer on the pipe wall. The thickness of this layer increases downward hence creating more resistance at the lower tube part which reduces the wall temperature compared to the top section.

It can also be deduced from the figures that there is gradual increase in the wall temperature as the heat input increases up to certain value when the performance limit of the pipe is reached. It can be seen that at the condenser section, the temperature of the 109W is higher than that of 101W showing that less energy is transferred to the cooling water when the pipe reaches its operation limit as shown in Figure 2.

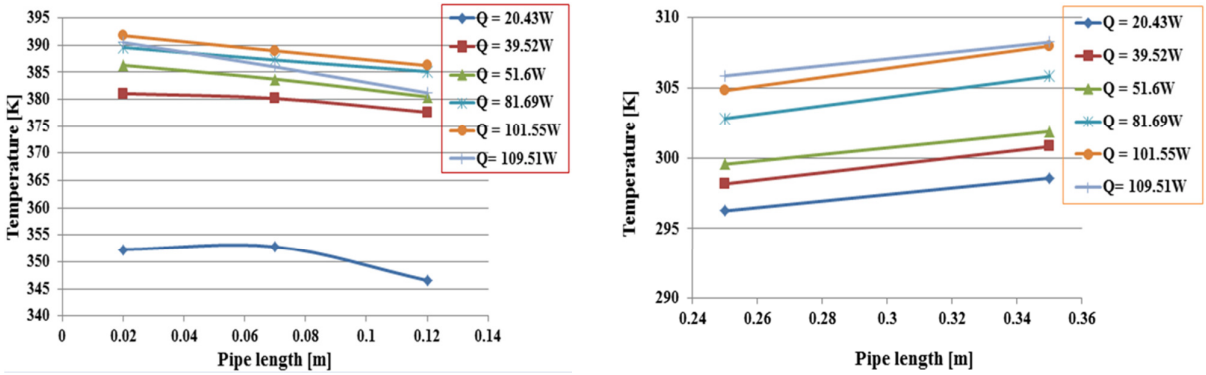

Fig. 3 Experimental temperature distributions on the evaporator and condenser sections of the thermosyphon, (left) Evaporator section, (right) Condenser section

Three different heat inputs; 31.18, 51.70 and 109.63W at constant average cooling water flow rate of 0.0021 kg/s were used in experimental investigation of the effects of inclining the thermosyphon heat pipe relative to the horizontal (10 to 90^{o}). Figure 4 shows the variation of the performance of the thermosyphon with the inclination angles at different heat inputs. It can be deduced from the figure that the heat transfer to the cooling water increases with the increase in the inclination in all the cases making 90^{o} the best. But the effects is more pronounced at small

heat input giving enhancement from 10° to 90° of 17.8%, 13.9% and 3.4% for 31.18W, 51.7W and 109W respectively. The effect of the inclination angles on the thermosyphon performance is caused by the gravitational force effects on the two-phase flow patterns, return of the condensate to the evaporator and the convective heat transfer coefficient.

The results shown in Figure 4 indicate that the inclination angle has an effect on the performance of the thermosyphon heat pipe, but this effect decreases as the heat input increases.

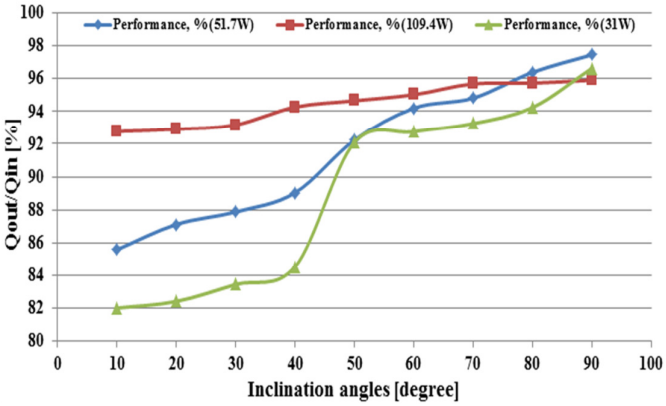

Fig. 4. Variation of the thermosyphon performance with inclination angle at different heat inputs

3. CFD Modelling

The aim of this section is to carry out a CFD analysis on the flow and heat transfer characteristics of a thermosyphon in both vertical and inclined orientations using VOF approach in ANSYSFLUENT 15.0. VOF is one of the models available in ANSYSFLUENT which is used for modelling two or more immiscible fluids by solving a single set of momentum equations and tracking the volume fraction of each fluid in the computational cell throughout the domain.

The motion of the working fluid inside a thermosyphon is described by continuity, momentum and energy equations. The continuity equation of the VOF for the secondary phase (*l*) is described as [30]

$$\nabla.\left(\alpha_l \rho_l \vec{u}\right) = -\partial/\partial t\left(\alpha_l \rho_l\right) + S_m \tag{5}$$

S_m, is the source term, used in the calculation of the mass transfer during evaporation and condensation. But for the primary phase, the continuity equation can be solved based on the constraint below

$$\sum_{l=1}^{n} \alpha_l = 1 \tag{6}$$

The energy equation is shared among the primary and secondary phases and is expressed as [30]:

$$\partial/\partial t(\rho E)+\nabla.\left[\vec{v}(\rho E+p)\right]=\nabla.(k_{eff}\nabla T)+S_E \tag{7}$$

S_E, is the energy source term for calculating the heat transfer during evaporation and condensation.

The momentum equation for the VOF can be written as [31]

$$\frac{\partial(\rho\vec{v})}{\partial t}+\nabla.\left(\rho\vec{v}\vec{v}\right)=-\nabla p+\nabla\left[\mu\left(\nabla\vec{v}+\nabla\vec{u}-\tfrac{2}{3}\mu\nabla.\vec{v}\,I\right)\right]+\rho g+F_v \tag{8}$$

where

$$\rho=\alpha_l\rho_l+\alpha_v\rho_v \tag{9}$$

$$k=\alpha_l k_l+\alpha_v k_v \tag{10}$$

$$\mu=\alpha_l\mu_l+\alpha_v\mu_v \tag{11}$$

$$E=\frac{\alpha_l\rho_l E_l+\alpha_v\rho_v E_v}{\alpha_l\rho_l+\alpha_v\rho_v} \tag{12}$$

$$E_l=C_{p,l}(T-T_{sat}) \tag{13}$$

$$E_v=C_{p,v}(T-T_{sat}) \tag{14}$$

F_v acts as the source term in the momentum equation given by [31]

$$F_v=\sigma_{lv}\frac{\alpha_l\rho_l k_v\nabla\alpha_v+\alpha_v\rho_v k_l\nabla\alpha_l}{0.5(\rho_l+\rho_v)} \tag{15}$$

where σ_{lv}, is the surface tension between the liquid and the vapour and k is the surface curvature.

A user-defined function (UDF) is used for calculating the mass and heat transfer between the liquid and vapour associated with the phase change processes. Both evaporation and condensation processes require two mass source terms for the liquid and vapour phases while heat transfer requires only one source term for the phases during evaporation and condensation. Mass and energy source terms in the continuity and energy equations respectively are defined in the UDF and linked to the FLUENT governing equations. Correlations proposed by De Schepper *et al.*, [14] for source terms are used in this work to calculate the mass and energy transfer as shown in Table 1.

Table 1
Correlations for mass and energy source terms [14]

Energy	Phase change	Temperature	State	Correlation
Mass	Evaporation	$T_m > T_{sat}$	Liquid	$S_m = -0.1\rho_l\alpha_l\frac{T_m - T_{sat}}{T_{sat}}$
			Vapour	$S_m = 0.1\rho_l\alpha_l\frac{T_m - T_{sat}}{T_{sat}}$
	Condensation	$T_m < T_{sat}$	Liquid	$S_m = 0.1\rho_v\alpha_v\frac{T_{sat} - T_m}{T_{sat}}$
			Vapour	$S_m = -0.1\rho_v\alpha_v\frac{T_{sat} - T_m}{T_{sat}}$
Heat transfer	Evaporation	$T_m > T_{sat}$		$S_E = -0.1\rho_l\alpha_l\frac{T_m - T_{sat}}{T_{sat}}LH$
	Condensation	$T_m < T_{sat}$		$S_E = 0.1\rho_v\alpha_v\frac{T_{sat} - T_m}{T_{sat}}LH$

3.1 Model Description and Validation

A 2D geometry of the 400mm long thermosyphon used in the experiment was developed in Gambit software to simulate the flow and heat transfer in the pipe using VOF approach. The simulation was carried out using COUPLED scheme for the pressure –velocity coupling, first order upwind for the momentum, volume fraction and energy while first order implicit is used for the transient formulation. The solution is considered to be converged when the residual scales of mass and velocity is below 10^{-4}. The gravity was taken as 9.81 m/s^2 in the y- axis for the vertical orientation cases. For the inclined heat pipe simulation, the gravitational force was determined on both x and y axes for each angle according to Figure 5 and the equations were updated in ANSYSFLUENT.

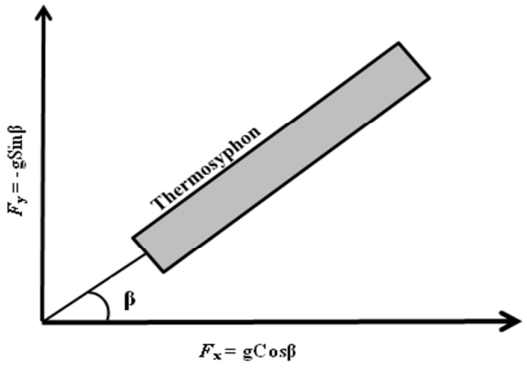

Fig. 5. Forces on an inclined thermosyphon heat pipe

Water-vapour and water-liquid are considered as primary and secondary phases respectively and phase interaction is defined in the surface tension force modelling using polynomial function of temperature (eq. 16) as derived using data from the steam table [15].

$$\sigma_{lv} = 0.09805856 - 1.845x10^{-5}T - 2.3x10^{-7}T^2 \quad (16)$$

where σ_{lv}, is the surface tension between the liquid and the vapour and T is the temperature shared by the phases.

The boiling temperature of 373K was considered at which the phase change occurred. The latent heat of 2455 kJ/kg was used in the UDF and the saturation temperature was taken as the average of the evaporator and condenser temperatures for each case as obtained from the experiment. Calculations were carried out with the time step size of 0.0005sec and number of time step between 120,000 and 180,000 depending on when the solution reaches a steady state (usually between 60 and 90 seconds).

Grid independence test was conducted by generating three different mesh sizes of 23,998, 38,278 and 120,794 cells in Gambit software and their properties are shown in Table 2. Temperature distributions along the wall of the pipe were monitored and shown in Figure 6 to test the grid independence of the results. The results show almost the same temperature distributions along the wall of the pipe for the mesh sizes of 38,278 and 120,794 cells. To reduce the computational time, the mesh size of 38,278 Quad, Map cells was used in the simulation of this work. Figure 7 shows the vapour volume fraction in the evaporator section indicating gradual generation of bubbles at different computational time. The top section (red colour) shows the presence of only vapour with volume fraction of one. Below such region there is mixture of vapour and liquid with blue colour indicating the liquid which has vapour volume fraction of zero. The liquid in the evaporator section is first heated and evaporation occurs when it reaches the boiling point leading to the bubbles generation which move to the condenser section. The vapour is condensed on the wall of the condenser due to the cooling applied to such wall and transport back to the evaporator section for the next cycle.

The boiling temperature of 373K was considered at which the phase change occurred. The latent heat of 2455 kJ/kg was used in the UDF and the saturation temperature was taken as the average of the evaporator and condenser temperatures for each case as obtained from the experiment. Calculations were carried out with the time step size of 0.0005sec and number of time step between 120,000 and 180,000 depending on when the solution reaches a steady state (usually between 60 and 90 seconds).

Grid independence test was conducted by generating three different mesh sizes of 23,998, 38,278 and 120,794 cells in Gambit software and their properties are shown in Table 2. Temperature distributions along the wall of the pipe were monitored and shown in Figure 6 to test the grid independence of the results. The results show almost the same temperature distributions along the wall of the pipe for the mesh sizes of 38,278 and 120,794 cells. To reduce the computational time, the mesh size of 38,278 Quad, Map cells was used in the simulation of this work. Figure 7 shows the vapour volume fraction in the evaporator section indicating gradual generation of bubbles at different computational time. The top section (red colour) shows the presence of only vapour with volume fraction of one. Below such region there is mixture of vapour and liquid with blue colour indicating the liquid which has vapour volume fraction of zero. The liquid in the evaporator section is first heated and evaporation occurs when it reaches the boiling point leading to the bubbles generation which move to the condenser section. The vapour is condensed on the wall of the condenser due to the cooling applied to such wall and transport back to the evaporator section for the next cycle.

Table 2
Mesh information

Mesh information	Run 2	Run 7	Run 8
Cells	23,988	38,278	120,794
Faces	47,463	75,716	235,893
Nodes	23,474	37,437	115,098
Cell zone	4	4	4
Face zone	14	14	14

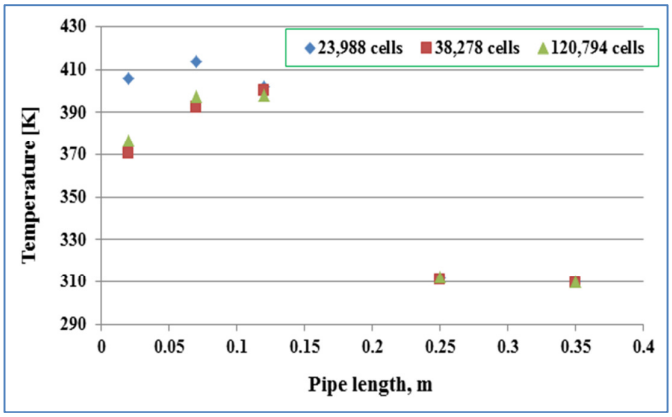

Fig. 6 Temperature distributions along the length of the thermosyphon for different mesh sizes

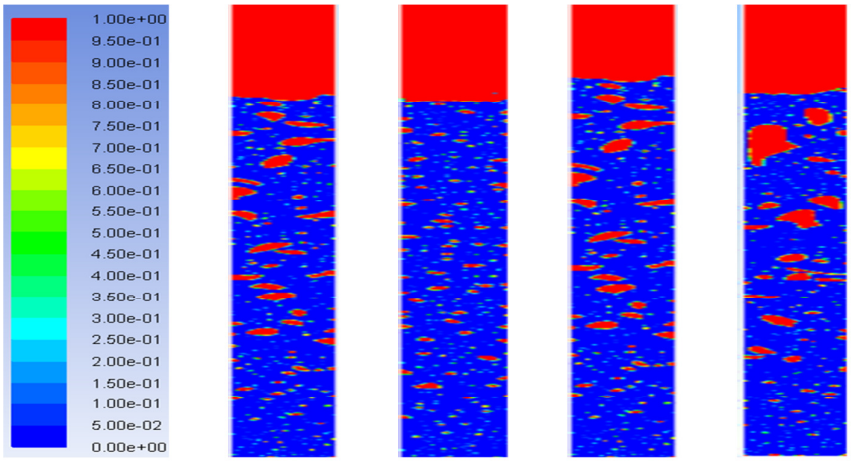

Fig. 7. Contours of vapour volume fraction at different computational time

The simulation was carried out at five different values of heat inputs of 39.5, 60.2, 81.7, 101.5 and 109.5 W applied to the evaporator section for the thermosyphon at the vertical position. While constant average heat inputs of 51.7W and 109.7W respectively were used for the inclination angles of 50° to 90°. Convective thermal condition was applied to the condenser section by specifying the heat transfer coefficient, h_c W/m^{2}K of the cooling water according to the following equation

$$h_c = \frac{Q_{out}}{\pi D L_{cond}\left(T_{cond} - T_{cw}\right)} \tag{17}$$

where *D* and L_{cond} are the pipe diameter and condenser length respectively. T_{cond} and T_{cw} are the average temperatures on the condenser wall and the cooling water respectively. All the parameters in equation 17 are obtained from the experiment and used to calculate the convective heat transfer coefficient for each case which is used in the ANSYSFLUENT as input. As part of the boundary conditions, the inner wall of the tube is considered as stationary and with no slip condition applied.

The CFD predicted temperature distributions on the thermosyphon wall is compared with the experimental results for different heat inputs when the pipe is at vertical position (90°) as shown in Figures 8 (a and b). The figure shows good agreement between the simulation and the experimental results for the various heat inputs with maximum deviation of ±4.2%. Figure 9 shows the variation of the thermal resistances with the selected heat inputs for both CFD and experiment with deviation of ±5.8%. Figures 8 and 9 indicate the validity of the CFD modelling technique used in this work.

Figures 10 (a and b) compare the predicted and measured temperature distributions for different inclination angles (50, 70 and 80°) and heat inputs of 51.7W and 109.7W with deviation ranging from ±1.2% to ±2.8%. Figure 11 compares the experimental and predicted thermal resistance at different inclination angles ranging from 50 to 90° with heat input of 109.7W. It can be seen from such figure that the lowest thermal resistance was reached at the 80° and 90° inclination angles.

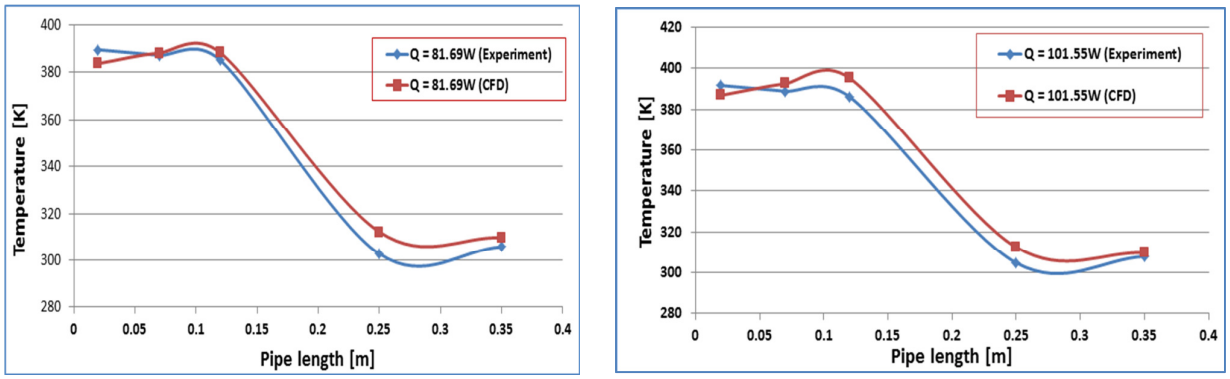

Fig. 8. Comparison of the experimental and CFD results for different heat inputs at vertical orientation, (left) Temperature distributions at Q = 81.69W, (right) Temperature distributions at Q = 101.55W

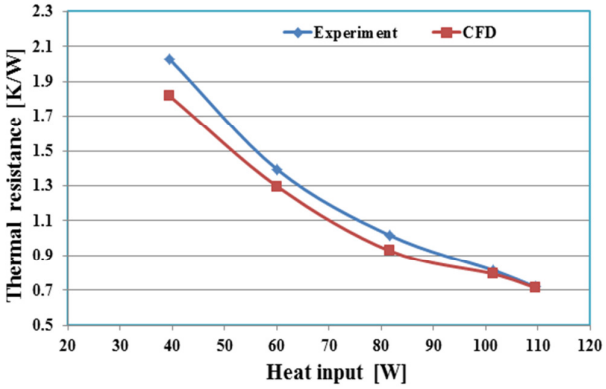

Fig. 9. Comparison of the predicted overall thermal resistance with experiment

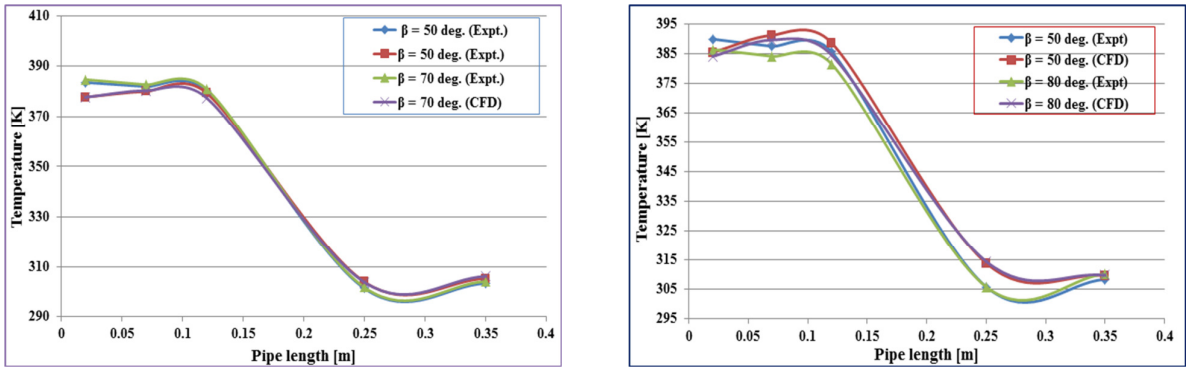

Fig. 10. Comparison of temperature distributions between experimental and CFD at different inclination angles for two different heat inputs, (left) Temperature profile for Q = 51.7W, (right) Temperature profile for Q = 109.7W

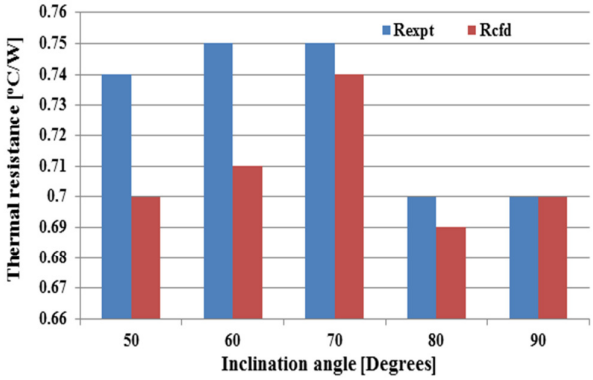

Fig. 11. Comparison of the overall thermal resistance between experimental and CFD results

4. Conclusion

In the present work, a CFD model was developed to simulate the evaporation and condensation processes in thermosyphon in vertical and inclined positions using together with UDF subroutines. For the first time, the effect of the thermosyphon inclination angle was incorporated in the modelling of thermosyphon by resolving the gravitational force in x and y axes. Experiments were carried out for wide range of operating conditions to study the effects of the heat input and the inclination angle on the thermosyphon performance. The results of the experiments were compared with that of the simulation and good agreement was found on the temperature distributions along the axial length of the pipe and the thermal resistance. Results of both CFD and experiments showed that as the heat inputs increases, the wall temperature on both evaporator and condenser section increase, while the thermal resistance decreases. The effect of the inclination angle was modelled and the predicted results were found to be in good agreement with the experimental ones. Experimental and numerical results showed that increasing the inclination angle will improve the thermosyphon heat pipe performance to reach its maximum value at 90o, but this effect decreases as the heat input increases. This work highlights that the complex evaporation and condensation processes in the thermosyphon heat pipe were successfully modelled and can be used to enhance the performance of thermosyphon heat pipes.

Acknowledgement
The first author acknowledged the financial support received from Kano University of Science and Technology, Wudil, Kano – Nigeria and Tertiary Education Trust Fund (TETFUND), Abuja – Nigeria.

References

[1] Peterson, George P. "An introduction to heat pipes: modeling, testing, and applications." (1994).
[2] Reay, David, Ryan McGlen, and Peter Kew. *Heat pipes: theory, design and applications*. Butterworth-Heinemann, 2013.
[3] Vasiliev, Leonard L. "Heat pipes in modern heat exchangers." *Applied thermal engineering* 25, no. 1 (2005): 1-19.
[4] Chow, T. T., Wei He, and Jie Ji. "Hybrid photovoltaic-thermosyphon water heating system for residential application." *Solar energy* 80, no. 3 (2006): 298-306.
[5] Abreu, Samuel Luna, and Sergio Colle. "An experimental study of two-phase closed thermosyphons for compact solar domestic hot-water systems." *Solar Energy* 76, no. 1-3 (2004): 141-145.
[6] Poulad, M. E., and Alan Fung. "Potential benefits from Thermosyphon-PCM (TP) integrated de-sign for buildings applications in Toronto." In *Proceedings of eSim: the Canadian conference on building simulation*, pp. 601-14. 2012.
[7] Hartnett, James P., Thomas F. Irvine, George A. Greene, and Young I. Cho. *Advances in heat transfer*. Vol. 31. Academic press, 1998.
[8] Japikse, D. "Advances in thermosyphon technology." In *Advances in Heat Transfer*, vol. 9, pp. 1-111. Elsevier, 1973.
[9] Chami, Nada, and Assaad Zoughaib. "Modeling natural convection in a pitched thermosyphon system in building roofs and experimental validation using particle image velocimetry." *Energy and Buildings* 42, no. 8 (2010): 1267-1274.
[10] Wongtom, Sompon, and Tanongkiat Kiatsiriroat. "Effect of inclined heat transfer rate on thermosyphon heat pipe under sound wave." *Asian Journal on Energy and Environment* 10, no. 04 (2009): 214-220.
[11] Alizadehdakhel, Asghar, Masoud Rahimi, and Ammar Abdulaziz Alsairafi. "CFD modeling of flow and heat transfer in a thermosyphon." *International Communications in Heat and Mass Transfer* 37, no. 3 (2010): 312-318.
[12] Asmaie, L., M. Haghshenasfard, A. Mehrabani-Zeinabad, and M. Nasr Esfahany. "Thermal performance analysis of nanofluids in a thermosyphon heat pipe using CFD modeling." *Heat and Mass Transfer* 49, no. 5 (2013): 667-678.
[13] Liu, Zhen-Hua, Yuan-Yang Li, and Ran Bao. "Thermal performance of inclined grooved heat pipes using nanofluids." *International journal of thermal sciences* 49, no. 9 (2010): 1680-1687.

[14] De Schepper, Sandra CK, Geraldine J. Heynderickx, and Guy B. Marin. "Modeling the evaporation of a hydrocarbon feedstock in the convection section of a steam cracker." *Computers & Chemical Engineering* 33, no. 1 (2009): 122-132.
[15] Fadhl, Bandar, Luiz C. Wrobel, and Hussam Jouhara. "Numerical modelling of the temperature distribution in a two-phase closed thermosyphon." *Applied Thermal Engineering*60, no. 1-2 (2013): 122-131.
[16] Zainal, S., C. Tan, C. Sian, and T. Siang. "ANSYS simulation for Ag/HEG hybrid nanofluid in turbulent circular pipe." *J. Adv. Res. Appl. Mech.* 23, no. 1 (2016): 20-35.
[17] Sinz, C., H. Woei, M. Khalis, and S. A. Abbas. "Numerical study on turbulent force convective heat transfer of hybrid nanofluid, Ag/HEG in a circular channel with constant heat flux." *J. Adv. Res. Fluid Mech. Therm. Sci.* 24, no. 1 (2016): 1-11.
[18] Abubakar, S., CS Nor Azwadi, and A. Ahmad. "The use of Fe3O4-H2O4 nanofluid for heat transfer enhancement in rectangular microchannel heatsink." *J. Adv. Res. Mater. Sci.* 23 (2016): 15-24.
[19] Huminic, Gabriela, and Angel Huminic. "Heat transfer characteristics of a two-phase closed thermosyphons using nanofluids." *Experimental Thermal and Fluid Science* 35, no. 3 (2011): 550-557.
[20. Jouhara, Hussam, Zaki Ajji, Yahia Koudsi, Hatem Ezzuddin, and Nisreen Mousa. "Experimental investigation of an inclined-condenser wickless heat pipe charged with water and an ethanol–water azeotropic mixture." *Energy* 61 (2013): 139-147.
[21] Chehade, A. A., H. Louahlia-Gualous, S. Le Masson, I. Victor, and N. Abouzahab-Damaj. "Experimental investigation of thermosyphon loop thermal performance." *Energy Conversion and Management* 84 (2014): 671-680.
[22] Noie, S. H., M. R. Sarmasti Emami, and M. Khoshnoodi. "Effect of inclination angle and filling ratio on thermal performance of a two-phase closed thermosyphon under normal operating conditions." *Heat transfer engineering* 28, no. 4 (2007): 365-371.
[23] Hahne, E., and U. Gross. "The influence of the inclination angle on the performance of a closed two-phase thermosyphon." In *Advances in Heat Pipe Technology*, pp. 125-136. 1982.
[24] Emami, MR Sarmasti, S. H. Noie, and M. Khoshnoodi. "Effect of aspect ratio and filling ratio on thermal performance of an inclined two-phase closed thermosyphon." *Iranian Journal of Science and Technology* 32, no. B1 (2008): 39.
[25] Karthikeyan, M., S. Vaidyanathan, and B. Sivaraman. "Thermal performance of a two Phase closed thermosyphon using aqueous solution." *Int. J. Eng. Sci. Technol* 2, no. 5 (2010): 913-918.
[26] Grooten, M. H. M., and C. W. M. Van Der Geld. "The effect of the angle of inclination on the operation limiting heat flux of long R-134a filled thermosyphons." *Journal of heat transfer*132, no. 5 (2010): 051501.
[27] Ong, K. S., and W. L. Tong. "Inclination and fill ratio effects on water filled two-phase closed thermosyphon." *Proceedings 10IHPS, Taiwan* (2011).
[28] Abdullahi, B., R. K. Al-dadah, S. Mahmoud, Kiyarash Rahbar, and A. O. Algareu. "Effect of slope angle and truncation level on heat pipe based Compound Parabolic Collector for Kano, Nigeria."
[29] Abdullahi, Bala, R. K. Al-Dadah, and S. Mouhmud. "Optical performance of double receiver compound parabolic concentrator." *Energy Procedia* 61 (2014): 2625-2628.
[30] Fluent, Ansys. "Theory Guide (Release 14.0)." *Multiphase Flows, ANSYS, Inc* (2011): 491e616.
[31] Yang, Zheng, X. F. Peng, and P. Ye. "Numerical and experimental investigation of two phase flow during boiling in a coiled tube." *International Journal of Heat and Mass Transfer* 51, no. 5-6 (2008): 1003-1016.